

CD31 is a key coinhibitory receptor in the development of immunogenic dendritic cells

Marc Clement^a, Giulia Fornasa^a, Kevin Guedj^a, Sanae Ben Mkaddem^b, Anh-Thu Gaston^a, Jamila Khallou-Laschet^a, Marion Morvan^a, Antonino Nicoletti^a, and Giuseppina Caligiuri^{a,1}

^aInstitut National de la Santé et de la Recherche Médicale (INSERM), U1148, Laboratory of Vascular Translational Science, Université Paris Diderot, Sorbonne Paris Cité, Faculté de Médecine, Site Xavier Bichat, and Département Hospitalo-Universitaire (DHU) Fibrosis, Inflammation, and Remodeling (FIRE), F-75018 Paris, France; and ^bINSERM, U1149, Centre de Recherche sur l'Inflammation, Équipes de recherche labellisées Centre National de la Recherche Scientifique, Université Paris Diderot, Sorbonne Paris Cité, Faculté de Médecine, Site Xavier Bichat, Laboratoire d'Excellence Inflammex, and DHU FIRE, F-75018 Paris, France

Edited by Ira Mellman, Genentech, Inc., South San Francisco, CA, and approved February 10, 2014 (received for review August 6, 2013)

CD31 is a transhomophilic tyrosine-based inhibitory motif receptor and is expressed by both dendritic cells (DCs) and T lymphocytes. Previous studies have established that the engagement of CD31 drives immune-inhibitory signaling in T lymphocytes, but the effect exerted by CD31 signaling in DCs remains elusive. Here, we show that CD31 is a key coinhibitory receptor on stimulated DCs, favoring the development of tolerogenic functions and finally resulting in T-cell tolerance. The disruption of CD31 signaling favored the immunogenic maturation and migration of resident DCs to the draining lymph nodes. In contrast, sustaining the CD31/SHP-1 signaling during DC maturation resulted in reduced NF- κ B nuclear translocation, expression of costimulatory molecules, and production of immunogenic cytokines (e.g., IL-12, IL-6), whereas the expression of TGF- β and IL-10 were increased. More importantly, CD31-conditioned DCs purified from the draining lymph nodes of ovalbumin-immunized mice favored the generation of antigen-specific regulatory T cells (CD25⁺ forkhead box P3⁺) at the expense of effector (IFN- γ ⁺) cells upon coculture with naive ovalbumin-specific CD4⁺ T lymphocytes *ex vivo*. Finally, the adoptive transfer of CD31-conditioned myelin oligodendrocyte glycoprotein-loaded DCs carried immune tolerance against the subsequent development of MOG-induced experimental autoimmune encephalomyelitis *in vivo*. The key coinhibitory role exerted by CD31 on DCs highlighted by the present study may have important implications both in settings where the immunogenic function of DCs is desirable, such as infection and cancer, and in settings where tolerance-driving DCs are preferred, such as autoimmune diseases and transplantation.

CD31 tolerance | NF κ B | Treg | EAE

Dendritic cells (DCs) have an essential function in initiating CD4⁺ T-cell responses by recognizing and presenting specific antigens associated with danger signals (1, 2). These signals contribute to conferring a fully mature, immunogenic phenotype to DCs, which is characterized by the up-regulation of MHC costimulatory molecules (e.g., CD40, CD86, CD80). The ensuing up-regulation of the chemokine (C-C motif) receptor type 7 (CCR7) receptor enables the migration of DCs to draining lymph nodes following the chemokine (C-C) motif ligand 21 (CCL21) gradient (3, 4). Finally, the fully matured DCs produce the proinflammatory cytokines IL-1 β , TNF, IL-12, and IL-6 (5). Importantly, DCs can also exert the opposite function by tolerizing T cells against self-antigen-directed immune responses, which is necessary to minimize autoimmune reactions. However, insufficient DC immunogenicity and excessive tolerance would favor the development of chronic infections and tumors. The immunogenic function of DCs depends on the balance between activating and inhibitory signals that occur at the time of DC maturation (2).

Elucidating the inhibitory receptors that are involved in the control of DC maturation would facilitate new interventional strategies to control autoimmune diseases. Despite intensive work in this area (6), the coinhibitory receptors involved in the control of DC immunogenic functions remain poorly understood.

Ig-like immunoreceptor tyrosine-based inhibitory motif (ITIM) receptors are thought to play an essential role in inhibiting the maturation of DCs (7).

Among the Ig-like ITIM receptors, we propose that CD31 (8, 9) (also known as PECAM-1) may play an important role in DC function because CD31 is constitutively expressed on these cells (10). Moreover, CD31 is essentially engaged by homophilic binding (11), which remarkably occurs between interacting cells of the innate and adaptive immune system.

The low-affinity, transhomophilic engagement of CD31 (11) triggers downstream inhibitory signaling (9), leads to the detachment of CD31⁺ lymphocytes from the cells of the innate immune system (12), and raises the activation threshold of lymphocytes via the phosphorylation of CD31 ITIMs and the recruitment of SH2 domain-containing tyrosine phosphatase (e.g., SHP-1, SHP-2) upon the engagement of the antigen receptor (13–16). Nevertheless, the role played by CD31 in maturing DCs remains to be elucidated.

Interestingly, it has been shown that during LPS-driven maturation, CD31 expression is consistently reduced on human monocyte-derived DCs (17–19) and endotoxin-induced septic shock is exaggerated in CD31^{-/-} mice (20, 21). In addition, autoimmune disease models dependent on antigen presentation are accelerated in the absence of CD31 (22, 23), suggesting that the effective presentation of the immunizing antigens involved in specific adaptive immune responses is favored by the absence of CD31.

Significance

Much is known about the costimulatory receptors that contribute to the full maturation of DCs, whereas the coinhibitory receptors that are involved in the control of DC maturation and the maintenance of peripheral tolerance remain largely unknown. This work reveals that CD31, a transhomophilic coreceptor constitutively expressed by resting DCs, has a key coinhibitory function. CD31 is lost by maturing DCs, and the absence of CD31 favors immunogenic maturation. In contrast, upholding CD31 signaling during maturation converts stimulated DCs into tolerogenic cells. These findings will likely have a substantial impact on immunology research, because knowledge of the immune modulation of DCs is important in immune homeostasis as well as in communicable and noncommunicable diseases, including infection, autoimmunity, and cancer.

Author contributions: M.C., A.N., and G.C. designed research; M.C., G.F., K.G., A.-T.G., J.K.-L., M.M., and G.C. performed research; S.B.M. contributed new reagents/analytic tools; M.C., A.N., and G.C. analyzed data; and M.C. and G.C. wrote the paper.

The authors declare no conflict of interest.

This article is a PNAS Direct Submission.

Freely available online through the PNAS open access option.

¹To whom correspondence should be addressed. E-mail: giuseppina.caligiuri@inserm.fr.

This article contains supporting information online at www.pnas.org/lookup/suppl/doi:10.1073/pnas.1314505111/-DCSupplemental.

Here, we demonstrate that the disruption of CD31 signaling favors the maturation and subsequent migration of antigen-loaded DCs to the draining lymphoid organs, driving more rapid and effective antigen-specific T-cell responses. In contrast, upholding the CD31/SH2 domain-containing tyrosine phosphatase-signaling pathway with an agonist peptide reduces the extent of maturation of the DCs, which become tolerogenic toward recall antigens both in vitro and in vivo.

Results

Disruption of CD31 Signaling Favors the Maturation and Accelerates the Migration of Antigen-Loaded DCs to the Draining Lymph Nodes.

One of the canonical features of DCs is their transport of antigens from tissues to draining lymph nodes. We therefore compared the activation-induced migration of DCs, using the FITC-painting assay, between CD31^{+/+} and CD31^{-/-} mice (Fig. 1). The number of total leukocytes (CD45⁺) and DCs (CD45⁺CD11c⁺) was similar in CD31^{+/+} and CD31^{-/-} mice (Fig. 1A). The maturation marker CD80 was consistently expressed by FITC⁺ DCs (Fig. 1B) regardless of the presence of CD31, but the number of FITC⁺ DCs that had reached the draining lymph node was significantly higher in the absence of CD31 (Fig. 1C), and this increase was not explained by the expansion of a particular DC subset (Fig. 1D and E). To assess whether the genetic deletion of CD31 affects DC migration, we evaluated the expression of CCR7 and the migratory response to CCL21 of bone marrow-derived DCs (BMDCs) derived

from CD31^{+/+} and CD31^{-/-} mice in vitro. As shown in Fig. S1, the expression of CCR7, as well as the magnitude of CCL21-induced migration of CD31^{-/-} DCs, was similar to that of CD31^{+/+} control DCs, regardless of the maturation state. Thus, the absence of CD31 does not increase the response of DCs to the CCL21 gradient but, rather, promotes DC migration indirectly via more efficient maturation upon LPS stimulation.

Indeed, the maturation of BMDCs [as detected by the acquisition of MHC class II (MHCII) and CD80 surface expression] was accompanied by a consistent reduction in CD31 surface expression (Fig. 2A). The extent of the maturation achieved by BMDCs was greater in the absence of CD31, as detected by an increased frequency of mature (CD86⁺CD80⁺) DCs upon stimulation with a suboptimal (100 ng/mL) amount of LPS (Fig. 2B). The expression level of additional maturation markers, such as MHCII and CD40, on the surfaces of mature (CD80⁺CD86⁺) DCs was higher in the absence of CD31 (Fig. 2C), and all four markers were consistently expressed at higher densities on CD31^{-/-} LPS-stimulated BMDCs (Fig. 2D). More striking was the production of inflammatory cytokines, which was enhanced three- to sixfold in the absence of CD31 in both unstimulated and LPS-stimulated BMDCs (Fig. 2E).

Maintenance of CD31 Signaling Thwarts DC Immunogenic Maturation.

CD31 signaling, which is triggered by transhomophilic interactions, depends on the establishment of membrane-proximal, cis-homophilic interactions (11) (e.g., CD31-molecule clusterization). CD31 signaling was thus artificially upheld in LPS-stimulated DCs by using a synthetic peptide derived from the membrane-proximal extracellular sequence of the molecule (16). This peptide was able to prevent the internalization of endogenous CD31 molecules, which was promptly observed upon LPS stimulation, and concomitantly favored the formation of stable CD31 clusters on the surface of the stimulated DCs (Fig. 3A and Fig. S2). Furthermore, the engagement of CD31 molecules at the DC surface by the peptide promoted CD31 signaling, as detected by the tyrosine phosphorylation of SHP-2 (24–26), to the same extent as antibody-mediated cross-linking of the endogenous CD31 molecules (Fig. 3B). Upholding the CD31/SH2 phosphatase signaling with this peptide modified DC maturation both quantitatively and qualitatively. The expression of the costimulatory molecules MHCII, CD86, CD40, and CD80 (Fig. 3C) and of the immunogenic cytokines IL-12 and IL-6 (Fig. 3D) was significantly reduced, whereas that of TGF- β 1 and IL-10 was increased. The measure of soluble cytokines in the culture supernatant confirmed the dichotomy between the effects exerted by CD31 signaling on the production of proinflammatory and anti-inflammatory cytokines (Fig. 3E).

Intracellular Coinhibitory Signaling Driven by CD31 Involves SHP-1 and Reduces NF- κ B Nuclear Translocation.

The CD31-dependent coinhibition of T cells involves the action of SHP-2 (24). To identify whether the activation of SHP-2 that accompanies CD31 signaling also plays a functional role in the CD31-dependent coinhibition of DCs, we examined the effect of phenylhydrazonopyrazolone sulfonate (PHPS1). High doses of PHPS1 were necessary to prevent the inhibitory effect of CD31 signaling on LPS-driven IL-6 production by BMDCs (Fig. 4A), suggesting that another SH2 domain-containing tyrosine phosphatase was involved in the coinhibitory signaling pathway downstream of CD31 in DCs. In addition to SHP-2, the ITIMs of CD31 can recruit and activate SHP-1 (13). Our data show that the CD31 coinhibition of DCs is indeed mediated by the activity of SHP-1, because low doses of sodium stibogluconate (SSG), which specifically inhibits SHP-1, were able to abolish the negative effect of CD31 signaling on IL-6 production (Fig. 4A). In addition, the peptide was ineffective in reducing IL-6 production by SHP-1^{-/-} BMDCs (Fig. 4B). SHP-1 has recently been highlighted as a key

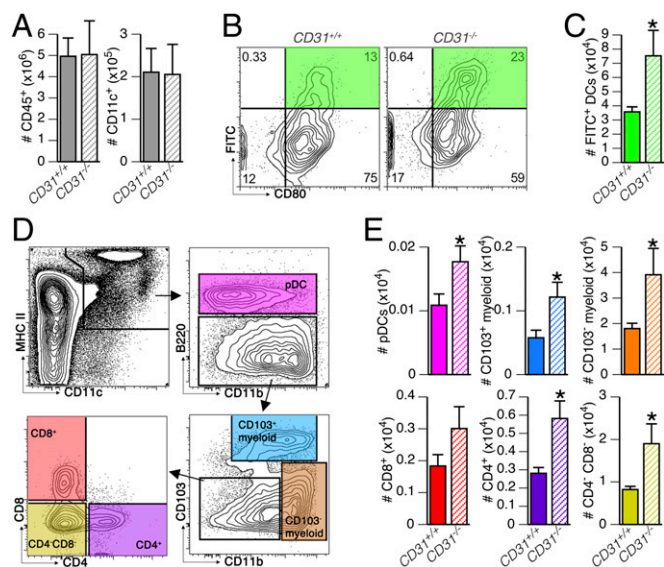


Fig. 1. Absence of CD31 favors DC migration to the draining lymph nodes. DC migration to the lymph nodes was evaluated with the FITC-painting assay in CD31^{+/+} mice and CD31^{-/-} littermates ($n = 6$ mice per group). (A) Absolute numbers of leukocytes (CD45⁺) and DCs (CD45⁺CD11c⁺) in lymph nodes were similar in CD31^{+/+} and CD31^{-/-} mice at steady state. (B) Representative contour plots show how the recent skin-derived and activated DCs were identified (FITC⁺CD80⁺) in the lymph nodes of CD31^{+/+} and CD31^{-/-} mice. (C) Number of FITC⁺ DCs in the draining lymph nodes of the CD31^{+/+} mice was significantly lower than that in the CD31^{-/-} mice. * $P < 0.05$ vs. CD31^{+/+}. (D) Gating strategy used to identify DC subsets in the lymph nodes: DCs (MHCII⁺CD11c⁺ cells) were identified as plasmacytoid by the expression of B220 [B220⁺, plasmacytoid DCs (pDCs)]; CD11b⁺B220⁻ cells were further subdivided into CD103⁺ and CD103⁻ myeloid DCs, and the remaining CD11b^{low} (lymphoid) DCs were classified as CD4⁺ or CD8⁺ single-positive DCs and CD4⁺CD8⁻ double-negative DCs. (E) Absolute number of the DC subsets described in D among FITC⁺ DCs. The analysis shows that FITC painting induces the recruitment of myeloid CD103⁻ and CD4⁻CD8⁻ double-negative lymphoid DCs in the draining lymph node. The absence of CD31 was associated with a generalized increase in FITC⁺ DCs, regardless of their subset. * $P < 0.05$ vs. CD31^{+/+}.

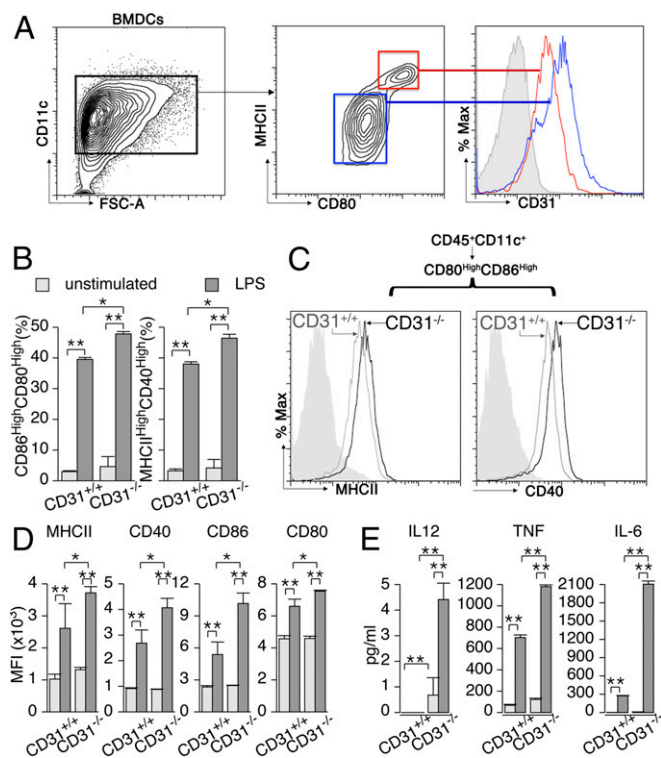


Fig. 2. CD31 expression on DCs is reduced in mature DCs, and a loss of surface CD31 favors DC maturation in response to LPS. BMDCs were obtained as described in *Materials and Methods*. (A) CD11c⁺ BMDCs were used for analysis upon stimulation with LPS (100 ng/mL, overnight). The expression of CD31 at the surface of mature (red lines, MHCII^{high}CD80^{high}) CD31^{+/+} BMDCs was consistently reduced compared with that of immature (blue lines, MHCII^{dim}CD80^{dim}) CD31^{+/+} BMDCs. The filled gray histogram represents CD31 staining on CD31^{-/-} BMDCs. %Max, percentage of maximum. (B) Stimulation with suboptimal LPS (100 ng/mL, overnight) led to a significantly greater percentage of mature (identified as CD86^{high}CD80^{high} or MHCII^{high}CD40^{high}) BMDCs in the absence of CD31. **P* < 0.05, ***P* < 0.01 vs. CD31^{+/+}. (C) Representative cytometry profile overlays show that the density of MHCII and CD40 was consistently higher in CD80^{high}CD86^{high} (mature) BMDCs (CD45⁺CD11c⁺) derived from CD31^{-/-} mice compared with those from CD31^{+/+} mice. (D) Quantification of the differences in the expression of MHCII, CD40, CD86, and CD80 by BMDCs (CD11c⁺) in response to LPS stimulation. All of the markers were significantly more abundant on LPS-stimulated CD31^{-/-} cells than on CD31^{+/+} cells. **P* < 0.05, ***P* < 0.01 vs. CD31^{+/+}. (E) In agreement with a greater expression of costimulatory molecules, CD31^{-/-} BMDCs also released greater amounts of soluble (in the supernatant) proinflammatory cytokines in response to LPS. Regarding surface costimulatory molecule expression, no differences were observed in terms of cytokine production between the two strains in basal (unstimulated) culture conditions. **P* < 0.05, ***P* < 0.01 vs. CD31^{+/+}. The data are expressed as the average \pm SEM of the MFI of each parameter obtained from five independent experiments (*n* \geq 3 mice per strain in all experiments); individual data were used for analysis.

molecule in the regulation of DC function (27), notably through the inhibition of the signaling pathway leading to the nuclear translocation of NF- κ B, a fundamental activation step downstream of LPS stimulation (28). The pharmacological inhibition of NF- κ B effectively blocked the phenotypic maturation of DCs (Fig. 4C), as expected. In agreement with its inhibitory function, the absence of CD31 resulted in an eightfold increased production of IL-6 compared with CD31^{+/+} cells. The effective inhibition of IL-6 production in these cells by the NF- κ B inhibitors suggested that CD31 coinhibitory signaling involves a regulatory step on NF- κ B translocation. Immunohistochemistry and cytometric analyses of nuclei preparations supported this hypothesis by showing that the CD31 peptide effectively reduces the extent of NF- κ B

p65 translocation to the DC nucleus during LPS stimulation (Fig. 4D–F). This process can explain, at least in part, why CD31 signaling results in the reduction of DC proinflammatory cytokines and costimulatory molecules.

Engagement of CD31 on DCs Affects Their Migration in Vivo. To assess whether CD31 engagement affects DC function in vivo, we first tracked the CD31 agonist in situ, after a single s.c. injection, by using a fluorescein-conjugated peptide (FAM-CD31 peptide) and immunofluorescence confocal microscopy. These experiments showed that the CD31 peptide effectively targets the CD11c⁺ cells (DCs) of the skin (Fig. 5A). Cytometric analysis of

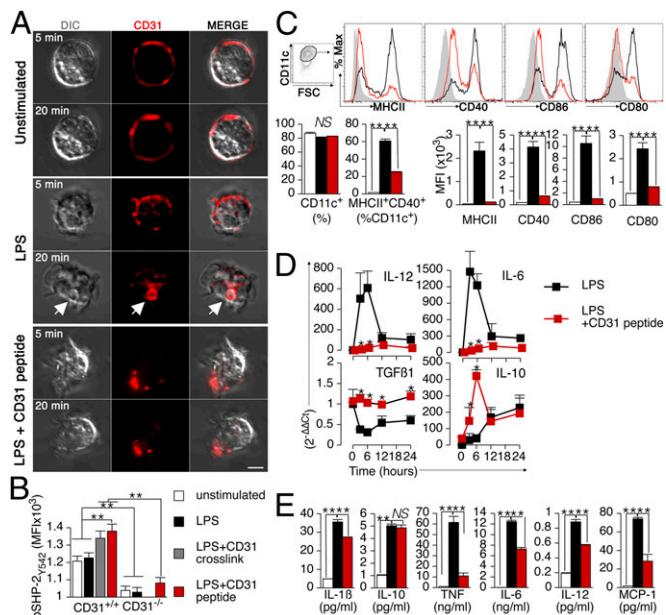


Fig. 3. CD31-driven inhibitory functions can be upheld in LPS-stimulated DCs using a homotypic CD31 peptide. (A) Representative images of confocal images of CD31 immunofluorescent staining on cultured BMDCs. Without LPS stimulation and in the absence of cell permeabilization, CD31 staining is exclusively detectable at the cell surface. LPS stimulation (1 μ g/mL) induces a rapid internalization of surface CD31 molecules, as detected after only 5 min of stimulation. CD31 molecule internalization is further evident and associated with the formation of intracellular vesicles (white arrow) after 20 min. The presence of the homotypic CD31 peptide prevents the internalization of endogenous CD31 molecules and, instead, favors their clustering at the cell surface (agglomerated red staining) on stimulated BMDCs. (Scale bar, 5 μ m.) (B) SHP-2 phosphorylation (pSHP-2_{Y542}), which is typically associated with CD31 outside-in signaling (25), was evaluated in BMDCs briefly stimulated with LPS (200 ng/mL for 15 min) in which CD31 signaling was either enhanced (LPS + CD31 cross-link and LPS + CD31 peptide) or invalidated (CD31^{-/-}). Of note, pSHP-2_{Y542} was consistently reduced in CD31^{-/-} DCs, whereas it was significantly increased upon antibody-mediated cross-linking as well as by the CD31 peptide only in CD31^{+/+} cells. These data indicate that the CD31 peptide 551–574 is a CD31 receptor agonist. ***P* < 0.01. (C) Cytometric analysis of MHCII, CD40, CD86, and CD80 expression on BMDCs incubated overnight with LPS (1 μ g/mL) revealed that upholding CD31 signaling with the CD31 agonist peptide (50 μ g/mL) results in reduced DC maturation, as detected by the reduction of costimulatory molecule expression levels. Filled histogram, no LPS; black line, LPS; red line, LPS + CD31 peptide. FSC, forward side scatter; NS, not significant. ***P* < 0.01. (D) Time course of proinflammatory and anti-inflammatory cytokine gene expression by real-time PCR showed that the CD31 agonist peptide significantly reduced the expression of IL-12 and IL-6, whereas it increased the expression of TGF- β 1 and IL-10 by LPS-stimulated BMDCs. The data are expressed as 2^{- $\Delta\Delta$ Ct} (43). (E) LPS-induced production of proinflammatory cytokines, but not of IL-10, by BMDCs was consistently reduced in the presence of the CD31 peptide. ***P* < 0.01. The data are from three separate preparations per condition. All of the experiments were repeated at least twice and provided similar results.

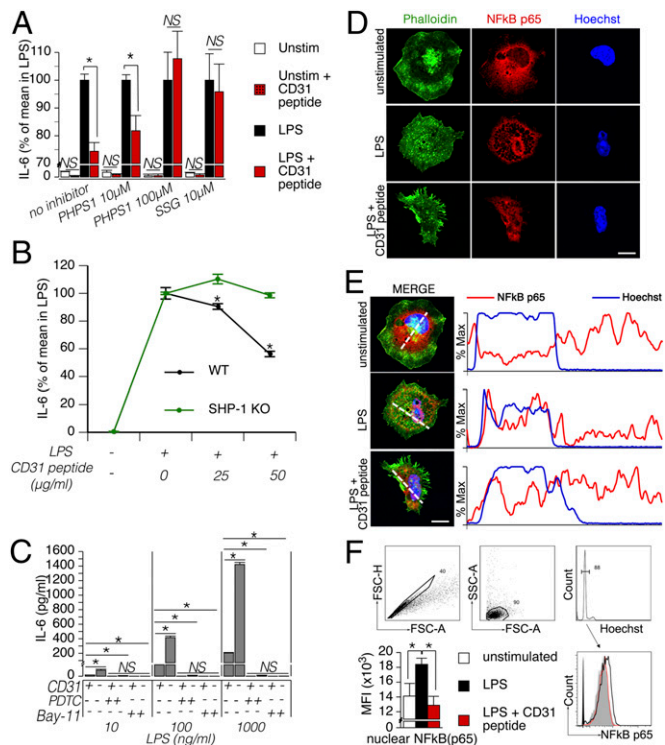


Fig. 4. CD31/SHP-1 signaling impairs LPS-driven NF- κ B nuclear translocation in DCs. (A) BMDCs (10^5 per condition) were preincubated for 30 min with SHP-1/2 inhibitors (10 μ M PHPS1, which specifically inhibits SHP-2; 100 μ M PHPS1, which inhibits both SHP-1 and SHP-2; and 10 μ M SSG, which specifically inhibits SHP-1) and subsequently supplemented with LPS (1 μ g/ml) and the CD31 peptide (50 μ g/ml) or vehicle. Unstimulated (Unstim) cells were used as a control. CBA analysis of IL-6 concentration in the supernatant of the different experimental conditions (expressed as a percentage of the mean values obtained in LPS-stimulated BMDCs) showed that CD31-driven signaling in DCs is mediated by SHP-1, because only low doses of SSG abolished the inhibitory effect of the CD31-agonist peptide on IL-6 production. $*P < 0.05$. (B) BMDCs derived from WT and SHP-1 $^{-/-}$ mice were stimulated with LPS (1 μ g/ml) with or without the CD31 peptide at the indicated concentration overnight. Analysis of IL-6 content in the supernatant of these experiments indicated that SHP-1 is essential for CD31 peptide activity. $*P < 0.05$. (C) Use of the NF- κ B inhibitors [20 μ M Bay 11, 50 μ M ammonium pyrrolidinedithiocarbamate (PDTC)] completely inhibited the production of IL-6 by both CD31 $^{+/+}$ and CD31 $^{-/-}$ LPS-stimulated BMDCs. NF- κ B inhibitors completely blocked IL-6 production by CD31 $^{-/-}$ cells despite the fact that these cells produced significantly greater amounts of the cytokine compared with CD31 $^{+/+}$ LPS-stimulated BMDCs, suggesting that CD31 may exert its coinhibitory effects on DCs by having an impact on NF- κ B activation. $*P < 0.05$. (D) Representative example of intracellular NF- κ B p65 immunofluorescent staining of fixed-permeabilized DCs based on confocal microscopic analysis. Phalloidin (green) and Hoechst (blue) counterstaining was used to localize the cell surface and the nuclei, respectively. NF- κ B p65 staining was concentrated in the nucleus of LPS-stimulated DCs, whereas the staining was only visible in the cytoplasm of unstimulated cells. Interestingly, the presence of the CD31-agonist peptide prevented this phenomenon; NF- κ B p65 distribution appeared diffuse in this condition. (Scale bar: 10 μ m.) (E) Maximal fluorescence intensity was evaluated for Hoechst (blue) and NF- κ B p65 (red) across the dotted white line. The percentage of maximal fluorescence intensity along the dotted lines traced in the "merge" images is displayed. (Scale bar, 5 μ m.) (F) Example of the cytometric analysis and gating strategy used for the cytometric analysis. Nuclear singlets were identified in the FSC-A/FSC-H and FSC-A/SSC-A scatter plots. G0/G1 nuclei were gated in the Hoechst fluorescence histogram and analyzed for NF- κ B p65 fluorescence signal. As shown in the histogram, the NF- κ B fluorescence profile of the nuclei derived from the LPS + CD31 peptide condition (red, open histogram) overlapped with that of the nuclei derived from unstimulated DCs (gray, filled histogram) and was shifted to the left compared with the fluorescence profile of LPS-stimulated DCs (black, open histogram). The statistical comparison of the maximal fluorescence intensity in the three conditions is shown on the right (the data are from three separate experiments). $*P < 0.05$.

the skin and draining lymph node cells 1 h after the injection showed that the CD31 peptide targets virtually all skin DCs and a small portion of lymph node DCs (Fig. 5B). The CD31 peptide mainly bound to the myeloid CD103 $^{-}$ and lymphoid CD8 $^{-}$ CD4 $^{-}$ DC subsets in the skin. A small percentage ($\sim 20\%$) of DCs within draining lymph nodes, mostly lymphoid DCs, were also positive for the presence of the FAM-CD31 peptide (Fig. 5C). To evaluate the effect of CD31 signaling on DCs involved in active immunization protocols, we evaluated the subsets of skin and draining lymph node DCs before and after immunization with complete Freund's adjuvant (CFA). As shown in Fig. 5D, CFA immunization induced the migration of myeloid CD103 $^{-}$ DCs from the skin to the draining lymph nodes. Of note, plasmacytoid DCs were enriched in the skin upon immunization, and this DC subset was particularly targeted by the fluorescent CD31 peptide, as shown in Fig. 5E. Interestingly, the FITC-painting assay was mainly associated with the migration of myeloid CD11b $^{+}$ CD103 $^{-}$ and lymphoid CD4 $^{-}$ CD8 $^{-}$ DCs from the skin to the draining lymph node, and upholding CD31 signaling with the agonist peptide actually reduced the percentage of migrating DCs in both of these main subsets (Fig. 5F).

Taken together, these findings suggest that CD31 signaling acts as a coinhibitory receptor that impairs the maturation and subsequent migration of DCs.

CD31-Conditioned DCs Redirect the Differentiation of Cognate CD4 $^{+}$ T Cells Toward a Regulatory Phenotype.

To assess whether the modification of the maturation phenotype and migration of the DCs obtained in the presence of the agonist CD31 peptide can affect subsequent DC function in eliciting antigen-specific T-cell responses, we evaluated the proliferation and intracellular cytokine production of naive ovalbumin (OVA)-specific CD4 $^{+}$ T cells cocultured with BMDCs that had been stimulated overnight with LPS and OVA in the presence of the CD31 peptide or the vehicle. The production of IL-2 by OT-II cells was considerably reduced in the presence of CD31-conditioned BMDCs compared with control BMDCs (Fig. 6A). In addition, CD31-conditioned BMDCs prevented the production of the effector cytokine by the OT-II cells (IFN- γ , as detected by intracellular cytokine staining; Fig. 6B).

We next aimed to evaluate whether similar modulatory effects of CD31 could affect the development of antigen-elicited immunogenic DCs in vivo. Toward this aim, we used ex vivo FACS-purified DCs derived from EGFP-transgenic (Tg) mice that were pretreated or not pretreated with the CD31 agonist peptide (termed "CD31 DC" henceforth) before OVA immunization in vivo. The FACS-purified DCs from the pooled draining lymph nodes (axillary and inguinal) were cocultured with purified naive (CD44 $^{-}$ CD25 $^{-}$ CD62L high) OT-II CD4 $^{+}$ T cells that were pre-treated with a violet cell-proliferation tracker [CellTrace Violet (CTV) Cell Proliferation Kit; Life Technologies]. The protocol is schematized in Fig. 6C. As shown in Fig. 6D, the proliferative response of OT-II CD4 $^{+}$ T cells was significantly reduced if the OVA antigen was presented by CD31 DCs. Interestingly, whereas the production of soluble IL-2, IFN- γ , and IL-17A followed the same trend as the proliferative response, IL-10 levels were unaltered in the supernatants of OT-II CD4 $^{+}$ T cells stimulated with CD31 DCs. Furthermore, the percentage and proliferation rate of regulatory T cells (Tregs), detected as CD25 high FoxP3 $^{+}$ OT-II CD4 $^{+}$ T cells, elicited by CD31 DCs were significantly increased (Fig. 6E). These results suggest that CD31 DCs can drive a tolerogenic T-cell response by skewing the differentiation of the cognate antigen-specific T cells toward a regulatory phenotype. The functional suppressive nature of CD31 DC-elicited Tregs was directly assessed in "cascade" experiments in which CD4 $^{+}$ CD25 high cells were purified from CD31 DC/OT-II T-cell cocultures and transferred to fresh cocultures of freshly purified spleen DCs with OT-II cells and OVA. As shown in Fig. 6F, CD31 DC-elicited CD4 $^{+}$ CD25 high cells suppressed the production of

IFN- γ and increased that of IL-10, supporting a functional regulatory phenotype acquired by antigen-specific T cells stimulated by CD31 DCs.

Adoptive Transfer of CD31-Conditioned DCs Significantly Delays the Development of Myelin Oligodendrocyte Glycoprotein-Driven Autoimmune Encephalomyelitis in Mice. We next used the BMDC adoptive transfer strategy with the myelin oligodendrocyte glycoprotein (MOG) peptides 35–55 to assess the effect of CD31-conditioned

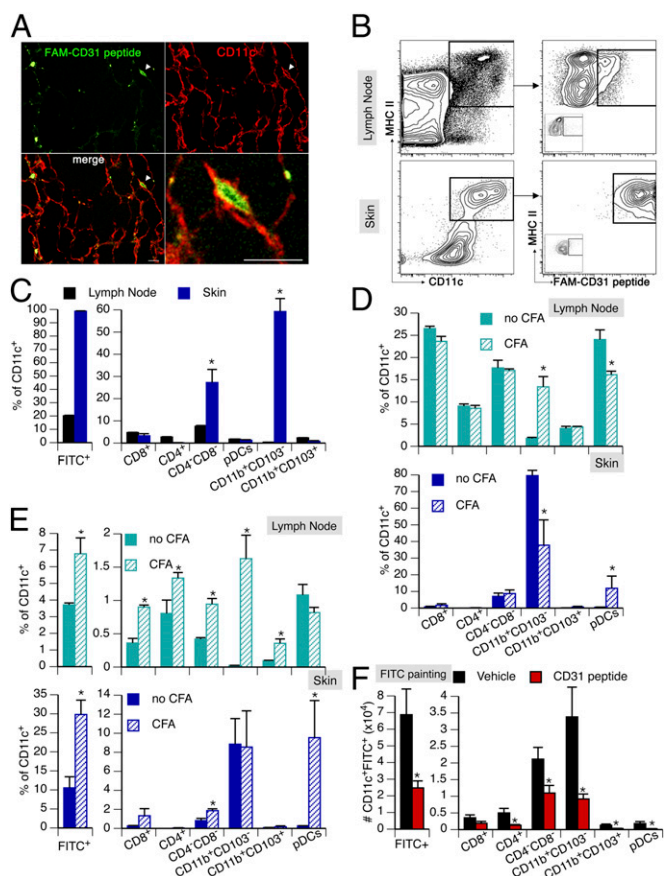


Fig. 5. CD31 peptide targets s.c. DCs. The potential targeting of resident DCs by the CD31 peptide injected in the s.c. space was tracked by confocal analysis and flow cytometry. (A) After the injection of a fluorescein-labeled (FAM, green) CD31 peptide by immunofluorescent staining of CD11c (red), s.c. DCs were identified in skin whole mounts. Several DCs were decorated with the CD31 peptide. The cell indicated by the arrowhead is displayed at a greater magnification. (Scale bars: 10 μ m.) (B) Flow cytometric analysis of FAM-CD31 peptide binding to DCs (CD11c⁺MHCII⁺) in the lymph node and skin of mice after s.c. injection. (C) Quantification, in the skin and draining lymph nodes, of the DC subsets that are targeted by the FAM-CD31 peptide 1 h after s.c. injection. A small number of lymph node DCs were positive for the FAM-CD31 peptide, mostly within the lymphoid subset. More importantly, virtually all of the skin DCs derived from the site of injection were targeted by the peptide. The main subsets of these DCs were myeloid CD103⁻ and lymphoid CD4⁺CD8⁺. **P* < 0.05. (D) DC subsets in the skin and draining lymph node before (no CFA) and 16 h after CFA immunization. CFA induced the migration of myeloid CD103⁻ DCs from the skin to the lymph nodes. **P* < 0.05. (E) Tracking of FAM-CD31 peptide-targeted DCs 16 h after CFA immunization in the skin and draining lymph nodes. In the draining lymph node, the percentage of FAM⁺ DCs was increased upon CFA immunization, including the enriched myeloid CD103⁻ DCs. In the skin, CFA immunization mainly induced the enrichment of pDCs (as shown in D); skin pDCs were targeted by FAM-CD31 peptide. **P* < 0.05. (F) Injection of the CD31 agonist peptide before FITC-painting assays reduced the number of FITC⁺ DCs reaching the draining lymph node. **P* < 0.05.

Clement et al.

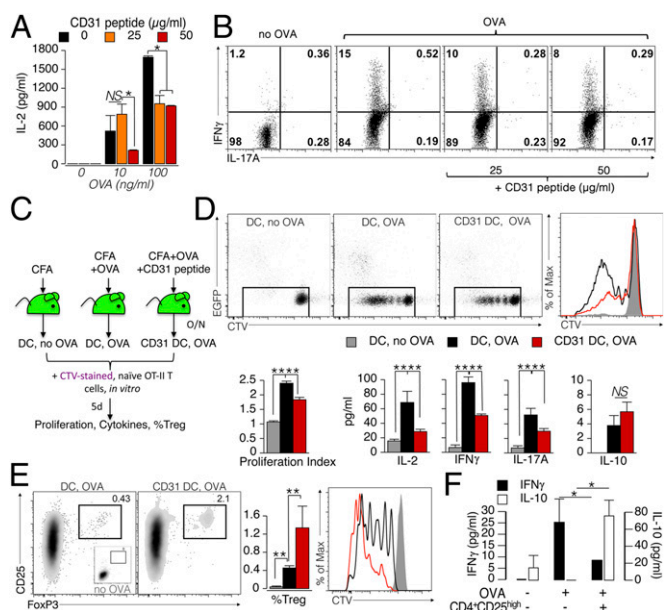


Fig. 6. CD31 signaling favors the development of tolerogenic DCs. (A) BMDCs (1×10^5) were matured overnight with LPS (100 ng/ml) in the presence of the CD31 peptide (25 or 50 μ g/ml). OVA peptide (10 or 100 ng/ml) was added during the last 4 h of LPS stimulation. The DCs were then washed and cocultured with naive (CD62L⁺) OT-II CD4⁺ T cells (5×10^5) for 4 d. A dose-dependent inhibition of IL-2 production by OT-II CD4⁺ T cells was exerted by CD31 peptide-conditioned DCs on cognate T cells. **P* < 0.05. (B) Representative dot plots display cytometric data of intracellular IFN- γ and IL-17A cytokine staining. Intracellular IFN- γ , which was readily increased in OT-II CD4⁺ T cells stimulated with OVA-loaded DCs, was reduced in a dose-dependent manner when the antigen was presented by CD31-conditioned DCs (DCs that had loaded the OVA antigen in the presence of the CD31 peptide). (C–F) Evaluation of the effect of CD31 signaling on DCs in vivo. (C) Experimental strategy (*n* = 3–5 per group). (D) Evaluation of CTV dilution showed that CD31 conditioning reduces the ability of DCs to elicit the proliferation of T cells. These results were confirmed by the lower production of IL-2, IFN- γ , and IL-17A, but not of IL-10. ***P* < 0.01. (E) CD31-conditioned DCs favored the differentiation and proliferation (CTV dilution) of CD4⁺ Tregs (CD25⁺FoxP3⁺) from naive OT-II CD4⁺ T cells. (F) Newly generated Tregs were fully competent in suppressing the production of effector cytokines by OT-II cells at a ratio of 1:10. Of note, the presence of these Tregs induced an increase in the amount of soluble IL-10. **P* < 0.05.

DCs on the development of autoimmune responses in vivo in the MOG-induced experimental autoimmune encephalomyelitis (EAE) model (Fig. 7). MOG-specific CD4⁺ T-cell clones that were elicited in mice receiving CD31 BMDCs produced less IL-2, IFN- γ , IL-17A, and IL-6 cytokines upon MOG-recall challenge in vitro, whereas the soluble levels of IL-4 and IL-10 in culture supernatants were not affected (Fig. 7A). In vivo tracking showed that CD31 BMDCs adoptively transferred by s.c. injection in the flanks of mice do reach the draining lymph nodes (axillary and inguinal), but in fewer numbers (Fig. 7B).

However, the blunted immune response observed following the transfer of CD31-conditioned DCs is not due merely to the lower number of DCs that reach the lymph node. Indeed, the adoptive transfer of either immature BMDCs or MOG-activated BMDCs did not affect the development of experimental EAE induced by MOG immunization in vivo. Instead, the clinical manifestations of the autoimmune response were consistently delayed in mice that had been adoptively transferred with CD31 DCs (Fig. 7C), which displayed significantly milder clinical signs of EAE than any other study groups for at least 3 d, suggesting that the DCs exerted a different effect than the endogenous cells. This issue was directly assessed in titration

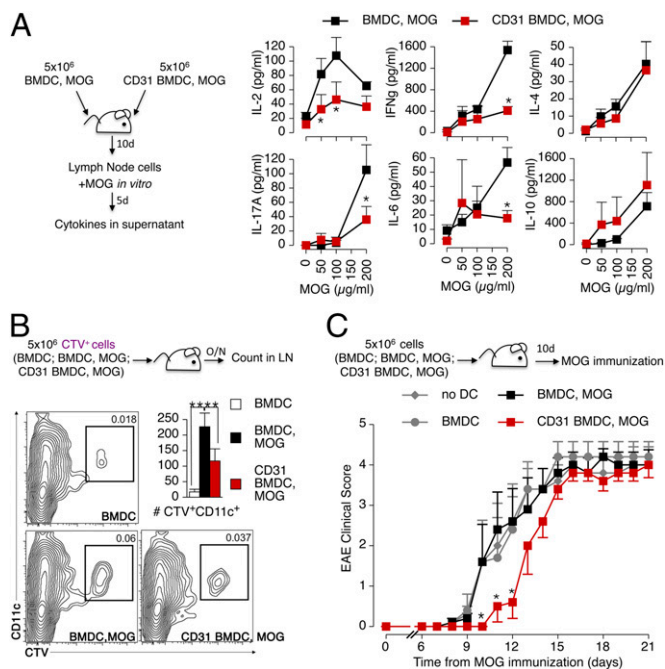


Fig. 7. CD31-conditioned BMDCs confer tolerance against autoimmune responses in vivo. (A) BMDCs and CD31-conditioned BMDCs (CD31 BMDCs) were stimulated with LPS overnight as described above, and MOG peptide 35–55 was added during the last 4 h. The cells were injected s.c. (total of 5×10^6 cells per mouse) in C57BL/6 mice. The draining lymph node cells of the recipient mice were harvested 10 d later and stimulated with increasing concentrations of the MOG peptide for 5 d in vitro. Cytokine release, analyzed by CBA in the supernatant, showed that CD31-conditioned BMDCs were not able to induce the production of IL-2, IFN- γ , IL-17A, and IL-6 by MOG-specific CD4⁺ T cells. Intriguingly, the production of IL-4 and IL-10 was similarly abundant in the two conditions. * $P < 0.05$. (B) Flow cytometry tracking of adoptively transferred CTV⁺ BMDCs, identified as CD11c⁺, showed that fewer CD31 BMDC, MOG cells reached the draining lymph nodes compared with BMDC, MOG cells. ** $P < 0.01$. (C) Potential tolerogenic properties of CD31 BMDC, MOG cells were evaluated in vivo by active MOG immunization 10 d after the adoptive transfer. The transfer of CD31 BMDC, MOG cells delayed the development of EAE. A minimum of three mice per group were used in each condition, and the experiments were repeated twice, with similar results. * $P < 0.05$.

experiments in which lower numbers of antigen-loaded BMDCs were adoptively transferred to experimental mice (Fig. 8A). As expected, reducing the number of injected antigen-loaded BMDCs results in milder antigen-specific T-cell proliferative and effector cytokine responses (Fig. 8B and C). However, only CD31-conditioned BMDCs concomitantly favored the enrichment of antigen-specific Tregs in the draining lymph node; the number of Tregs remained low in the lymph nodes of mice receiving OVA-loaded BMDCs at all of the tested cell dilutions (Fig. 8D). Finally, we observed that the adoptively transferred BMDCs exerted their effect directly, as detected with CTV-labeled BMDCs in GFP-Tg mice and with subsequent DC purification and functional testing in vitro (Fig. 8D). As expected, only exogenous BMDCs were able to elicit the production of effector cytokines in functional tests, provided that they had not been conditioned with CD31.

Discussion

CD31 is an important, yet neglected, immune inhibitory receptor (8, 9, 29). Because of its extracellular Ig-like domains and localization in the lateral junctions between endothelial cells in the vasculature (30), CD31 was initially viewed as a putative cell-adhesion molecule, and the ability of CD31-targeting antibodies or recombinant proteins (31, 32) to inhibit leukocyte transmigration

has long supported this perception. However, the absence of CD31 does not reduce the transmigration of blood leukocytes (33) but, rather, promotes CD4⁺ T-cell recruitment at inflammatory sites (23).

Several subsequent experimental studies have clearly demonstrated that CD31 plays important inhibitory signaling roles in effector-adaptive immune cells, such as T and B lymphocytes (14, 15, 24, 34–37). More recent studies have suggested that the homophilic engagement of CD31 between DCs and cognate T cells may establish the threshold for T-cell activation and tolerance (35), but the role played by this ITIM receptor in DC function has remained elusive.

In this study, we show that CD31 acts as a key coinhibitory receptor and dramatically modulates the function of DCs, independent of its already known regulatory function on other immune effectors. Whereas the reduction of CD31 molecules at the cell surface is a prerequisite for the immunogenic potential of DCs because it favors their maturation, accelerates their migration to the lymph nodes, and increases their production of proinflammatory cytokines, upholding CD31 signaling thwarts the immunogenic functions of DCs, instead favoring the generation and expansion of regulatory cognate T cells at the expense of the effector phenotype.

Interestingly, our data suggest that the engagement of surface CD31 on DCs is a key trigger for the regulatory signaling cascade that is mediated by SHP-1 and modulates NF- κ B activation and cytokine production (27).

The identification of the role played by CD31 during DC maturation in this study may thus have a broad impact in several research fields in immunobiology, wherever the immunogenic function of DCs is desirable or unwanted. For instance, the fact that CD31 surface expression is reduced on human DCs upon their interaction with LPS (17–19) and/or bacterial proteolytic enzymes (38) suggests that the invalidation of this coinhibitory receptor is necessary for the development of protective adaptive immune responses against bacteria. Similarly, interventional tools able to invalidate CD31 signaling may enhance the success of vaccination therapies in cancer. Indeed, the acquisition of CD31 by tumor cells (39) might be one mechanism by which tumor cells can engage the CD31 molecules of DCs, leading to a blunted immunogenic potential of DCs and, consequently, a flawed immune defense against cancer.

Materials and Methods

Mice. C57BL/6J (CD31^{+/+}) and OT-II [C57BL/6-Tg(Tcr α Tcr β)425Cbn/Crl] mice were purchased from Charles River France Laboratories. Breeding pairs of GFP-Tg mice [C57BL/6-Tg(ACTbEGFP)10sb/J] were kindly provided by R. Golub (Institut Pasteur, Paris) and maintained in a heterozygous state in our facility. Breeding pairs of CD31^{-/-} mice (33) on the C57BL/6J background were kindly provided by D. K. Newman (Milwaukee Blood Center, Milwaukee, WI). Homozygous SHP-1^{-/-} mice, generated and maintained in a colony as previously described (40), were a kind gift from Renato Monteiro (Inserm U699, Paris). The mice were maintained in our facility under an alternating 12-h light/12-h dark cycle in microisolator cages (four or fewer mice per cage) under specific pathogen-free conditions with free access to food and water. All investigations conformed to Directive 2010/63/EU of the European Parliament, and formal approval was granted by the local animal ethics committee (Comité d'éthique Bichat-Debré, Paris).

FITC-Painting Assay. The draining lymph node DCs were analyzed after FITC skin painting as described previously (41). Briefly, FITC (isomer 1; Sigma-Aldrich) was dissolved (8 mg/mL) in a 50:50 (vol/vol) acetone-dibutyl phthalate mixture just before application. This FITC solution was distributed in six spots (25 μ L per spot) on the shaved back skin of anesthetized mice. Mice treated with the CD31 peptide were injected s.c. with 100 μ g per mouse in four spots 1 h before FITC painting. Twenty hours later, the draining lymph nodes (inguinal, brachial, and axillary) and non-draining lymph nodes (popliteal) were removed (the left and right lymph nodes from each mouse were analyzed separately) and placed in a collagenase D (Roche) solution (1 mg/mL in RPMI) for 30 min. The enzymatic digestion was stopped by the addition of

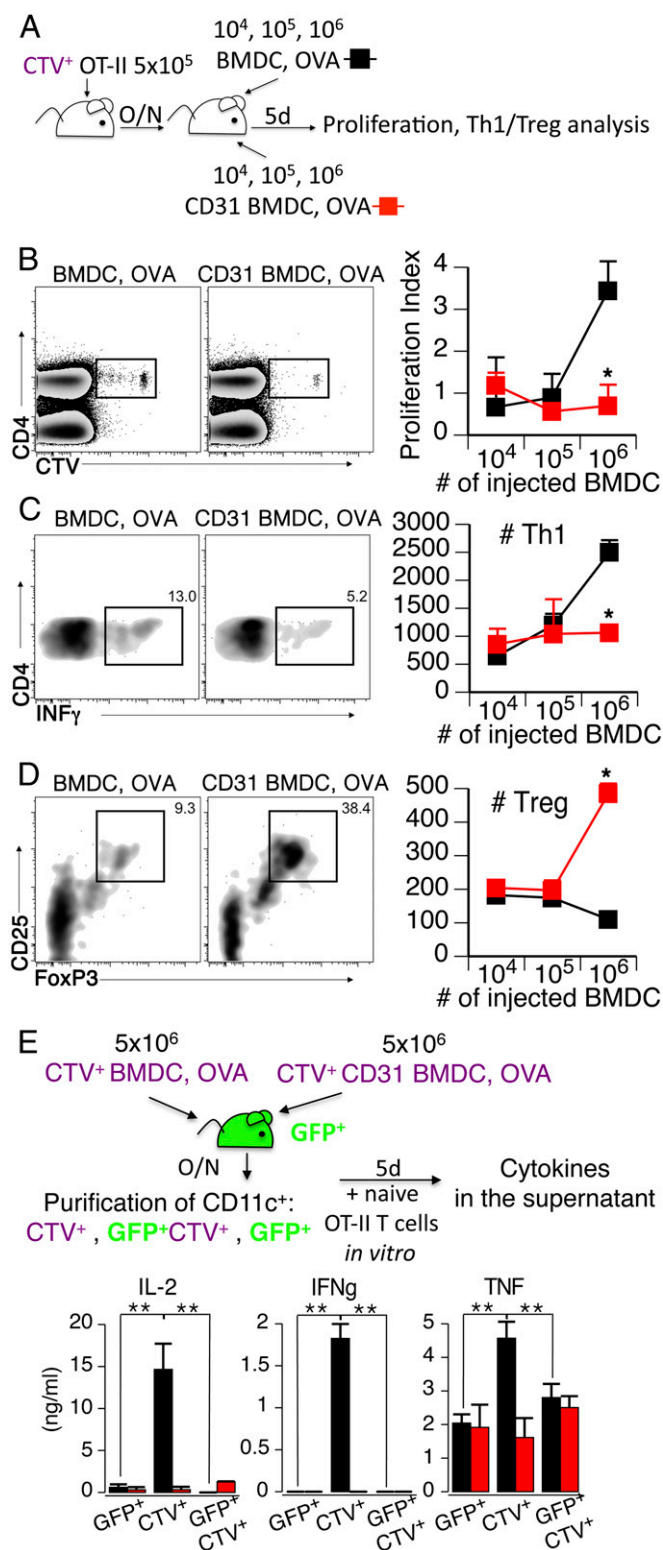


Fig. 8. Tolerance carried by CD31-conditioned BMDCs is supported by the induction of CD4⁺ Tregs in vivo. (A) CTV-labeled CD4⁺ naive OT-II (CTV⁺ OT-II) cells were transferred to C57BL/6 mice. On the following day, recipient mice received OVA-loaded BMDCs or CD31-conditioned BMDCs at the indicated number. Five days later, lymph nodes were harvested and processed for CTV dilution (proliferation) and T helper 1 (Th1)/Treg analysis by intracellular cytometry. O/N, overnight. (B) Proliferation of CTV⁺CD4⁺ cells is dependent on the number of adoptively transferred antigen-loaded BMDCs. Administration of CD31-conditioned BMDCs results in a low-magnitude, antigen-specific, T-cell proliferative response, regardless of the number of injected cells.

100 mM EDTA. The lymph nodes were then meshed through a 70- μ m filter. The cells were washed, pelleted, and stained before data acquisition and analysis by flow cytometry.

Induction and Maturation of BMDCs. BMDCs were induced from bone marrow cells of CD31^{+/+}, CD31^{-/-}, or SHP1^{-/-} mice by flushing the femurs of 6- to 10-wk-old mice with PBS (42). Pooled cells from six to eight femurs were washed in Iscove's modified Dulbecco's medium (IMDM; Life Technologies) and plated in 10-cm \emptyset Petri dishes (2×10^6 cells per dish) with IMDM supplemented with 15% (vol/vol) FCS, 10^{-5} M β -mercaptoethanol, 2 mM L-glutamine, 1 \times antibiotic/antimycotic solution, and supernatant from a GM-CSF-expressing cell line (J558-GM-CSF, a kind gift from S. Amigorena, Institut Curie, Paris; GM-CSF final concentration of 30 ng/mL). The supplemented medium was replaced every 3 d. Maturation assays were performed with nonadherent and loosely adherent cells, which were harvested between the eighth and 12th days of the culture and plated in 24-well plates overnight in the presence of LPS (from *Escherichia coli* O55:B5; Sigma) with or without CD31 peptide [amino acids 551–574, molecular weight of 2,606.0, provided as >95% pure by Genosphere or Mimotopes, with low endotoxin (<0.01 ng/ μ g, based on the limulus amoebocyte lysate test) and dissolved at 1 mg/mL in sterile 0.5% PBS/DMSO] at the indicated concentrations. Cells at the indicated densities were preincubated with inhibitors [NF- κ B inhibitors (20 μ M Bay 11-7821 and 50 μ M PDTC) from TOCRIS Bioscience and PTP Inhibitor V (PHP51, to inhibit SHP-2) and SSG (to block SHP-1) from Merck Millipore] for 30 min before LPS stimulation.

Cytokine Quantification. Cytokines were quantified using cytometric bead array (CBA) mouse kits and flex sets (IL-2, IL-4, IL-6, IFN- γ , TNF, IL-17A, IL-10, IL-1 β , IL-12, and MCP-1) following the manufacturer's protocols (BD Biosciences).

Analysis of Gene Expression by Real-Time PCR. BMDCs were seeded on 96-well, round-bottom plates at 1×10^5 cells per well. CD31 peptide and LPS were added at different time points as indicated. Total RNAs were extracted using TRIzol (Life Technologies), and mRNA reverse transcription was performed using iScript reverse transcriptase (Bio-Rad). Real-time PCR was performed on a CFX 100 (Bio-Rad) cyclo using the primers listed in Table 1, 1 ng of cDNA from each sample in a total volume of 22 μ L containing the forward and reverse primers (250 nM each), and SYBR Green Master Mix (Bio-Rad). The amplification program was as follows: one cycle at 50 $^{\circ}$ C for 2 min, one cycle at 95 $^{\circ}$ C for 15 min, and 50 cycles at 95 $^{\circ}$ C for 40 s and 60 $^{\circ}$ C for 1 min. Dissociation curves were analyzed at the end of the amplification, and data concerning the genes of interest were normalized by the expression of the β -actin gene in the same condition and were expressed compared with a control condition with no LPS and no CD31 peptide. The $2^{-\Delta\Delta C_t}$ formula described by Pfaffl (43) was applied, where threshold cycle (Ct) values correspond to the cycle at which the PCR enters the exponential phase.

Immunofluorescence Microscopy. CD31⁺ BMDCs were harvested 8 d after their differentiation, plated on Ibidi eight-well μ -Slides (2×10^5 cells per well), and allowed to adhere overnight. After careful washing, adherent cells were precooled on ice for 30 min and stained with an anti-mouse CD31 antibody [clone Mec13.3, directly coupled to phycoerythrin (PE)] for 30 min on ice. Thereafter, the cells were washed in ice-cold PBS and warmed up to 37 $^{\circ}$ C with complete medium containing or not containing LPS (1 μ g/mL) and the CD31 peptide (100 μ g/mL). The cells were allowed to stabilize for 5 min before image acquisition.

* $P < 0.05$. (C) Number of CTV⁺CD4⁺IFN- γ ⁺ (#Th1) cells elicited by the adoptive transfer of 1×10^6 CD31 BMDC, OVA cells was significantly lower than that elicited by BMDC, OVA cells at the same cell dilution. * $P < 0.05$. (D) Number of CTV⁺CD4⁺CD25⁺FoxP3⁺ (#Treg) elicited by the adoptive transfer of 1×10^6 CD31 BMDC, OVA cells was significantly higher than that elicited by BMDC, OVA cells at all tested cell dilutions. * $P < 0.05$. (E) Evaluation of the direct and indirect effects of CTV-labeled BMDCs adoptively transferred to GFP-Tg mice was performed by assessing the properties of FACS-purified DCs. Adoptively transferred BMDCs (CTV⁺) were able to elicit an antigen-specific immune response (production of IL-2, IFN- γ , and TNF), whereas endogenous DCs (GFP⁺) were ineffective, regardless of their positivity for CTV (possibly indicating the phagocytosis of exogenous BMDCs). As before, CD31 BMDCs did not elicit an antigen-specific response in terms of effector cytokine production. At least three mice per group were used in these experiments, which were repeated twice, with similar results. ** $P < 0.01$.

Table 1. Primers used to analyze the expression of cytokine and housekeeping genes

Gene	Forward primer	Reverse primer
mIL-6	AGTTGCCTTCTTGGGACTGA	TTCTGCAAGTGCATCATCGT
mIL-12	ATGACCCCTGTGCCTTGGTAG	CAGATAGCCCATCACCCCTGT
mIL-10	TGCCAAGCCTTATCGGAAAT	TTTTCACAGGGGAGAAATCG
mTGF- β 1	TGCGCTTGACAGATATAAAA	CTGCCGTACAACCTCCAGTGA
m β -Actin	TGTTACCAACTGGGACGACA	GCTGGGGTGTGAAGGTCTC

m, murine.

NF- κ B. BMDCs (2×10^5) were carefully washed, resuspended, and stimulated for 30 min at 37 °C in FCS-free medium with LPS (250 ng/mL) with or without the CD31 peptide (50 μ g/mL). Unstimulated cells were used as a control. At the end of the stimulation, the cell suspensions were layered onto polylysine-coated coverslips and allowed to adhere for 30 min at 37 °C. The coverslips were then washed twice with warm FCS-free medium, and the adherent cells were fixed with PBS/4% (wt/vol) paraformaldehyde (PFA; 15 min at room temperature) and incubated for 10 min with glycine (100 mM in PBS, pH 7.4) to quench residual aldehydes. The cell and nuclear membranes were then permeabilized with PBS/0.5% Triton X-100 for 10 min and extensively washed in PBS/0.5% Triton X-100/1% BSA before incubation with purified polyclonal rabbit anti-mouse NF- κ B p65 antibody (no. ab16502, Abcam; diluted at 5 μ g/mL in PBS/0.5% Triton X-100/1% BSA) for 90 min at room temperature. The coverslips were then extensively washed with PBS/0.5% Triton X-100/1% BSA and incubated for 30 min with 7.5 μ g/mL TRITC-conjugated AffiniPure F(ab')₂ Fragment Rabbit Anti-Goat IgG, Fc Fragment-Specific (no. 305-026-008; Jackson ImmunoResearch Laboratories) and 1 unit of Alexa Fluor 488 Phalloidin (Life Technologies) diluted in the same buffer. After extensive washing, the cells were incubated for 5 min with 1 μ g/mL Hoechst 33342 (Life Technologies) in PBS, washed twice in PBS, and cover-mounted with ProLong Gold Antifade Reagent (Life Technologies) before image acquisition.

Digital images were acquired using AxioVision software and a Zeiss Axio Observer Z1 microscope equipped with an ApoTome. Fluorescence-intensity analysis of the digital images was performed using ImageJ (National Institutes of Health).

Immunogenic Function of BMDCs. BMDCs (1×10^5) were incubated overnight with LPS (1 μ g/mL) with or without the CD31 peptide at the indicated concentration and loaded with increasing doses of OVA 323–339 peptide (AnaSpec) during the last 4 h. After the incubation period, the cells were thoroughly washed and cocultured with 5×10^5 naive OT-II CD4⁺ T cells (isolated from spleen and lymph node single-cell suspensions by magnetic cell sorting using a CD4⁺CD62L⁺ T Cell Isolation Kit II; Miltenyi Biotech). Four days later, the supernatant was collected for IL-2 analysis (CBA), and the cells were detached and subjected to intracellular flow cytometry analysis using a Mouse Th1/Th2/Th17 Phenotyping Kit (BD Biosciences).

In separate experiments, GFP-Tg mice were adoptively transferred with CTV-labeled BMDCs (5×10^6 per mouse by intradermal injection). To achieve this aim, BMDCs were prepared as previously described and stimulated overnight with LPS (1 μ g/mL) in the presence of OVA protein (30 μ g/mL, no. A5503; Sigma) and with or without the CD31 peptide (100 μ g/mL). The mice were euthanized after an overnight period, and the lymph nodes draining the site of injection were harvested and digested in collagenase D (1 mg/mL final concentration; Roche). Single-cell suspensions were washed and incubated with an anti-mouse CD11c antibody (clone HL3, PE-CF594; BD Biosciences) for 30 min on ice in PBS. The cells were then washed and submitted for FACS purification, yielding three populations of CD11c⁺ DCs: GFP⁺CTV⁻, GFP⁺CTV⁺, and GFP⁻CTV⁺. Naive (CD62L⁺CD25⁻) CD4⁺ T cells were FACS-purified from the spleens of OT-II mice. FACS-purified DCs and T cells were extensively washed and cocultured in V-bottom, 96-well plates (5×10^3 DCs and 50×10^3 CD4⁺ T cells, 1:10 ratio) for 5 d. At the end of the coculture, the supernatant was harvested and processed for cytokine content analysis using CBA technology.

Fluorescent Tracking of the CD31 Peptide. A total of 50 μ g of 5,6-FAM-conjugated CD31 peptide in 50 μ L of PBS was injected s.c. into the shaved abdomen of C57BL/6 mice. For whole-mount confocal analysis, the mice were killed under anesthesia 1 h later and skin coupons around the injection site (1 cm ϕ) were excised, rinsed in ice-cold PBS (2 mL for 20 min with orbital shaking repeated three times), and fixed in ice-cold PFA (2 mL for 20 min with orbital

shaking). The samples were then permeabilized in PBS/2% (vol/vol) Triton X-100/20% (vol/vol) DMSO/2% (vol/vol) BSA on ice for 1 h. The samples were then incubated for 48 h with the primary antibodies (Armenian hamster anti-mouse CD11c antibody, clone N418, Abcam; Syrian hamster anti-mouse podoplanin antibody, clone 11-033, AngioBio) and diluted in the same buffer at a final concentration of 20 μ g/mL each. After three washes (30 min each) in PBS/2% (vol/vol) Triton X-100/20% (vol/vol) DMSO, secondary antibodies [AffiniPure F(ab')₂ fragments, TRITC-conjugated anti-Armenian hamster IgG and DL649-conjugated anti-Syrian hamster IgG; both from Jackson ImmunoResearch] were diluted at 2 μ g/mL in PBS/2% (vol/vol) Triton X-100/20% (vol/vol) DMSO/2% (vol/vol) BSA and incubated with the samples overnight. Finally, the samples were extensively washed in PBS/2% (vol/vol) Triton X-100/20% (vol/vol) DMSO, cleared, and mounted as previously described for whole-mount mouse embryos (44). Digital images were acquired using AxioVision software and a Zeiss Axio Observer Z1 microscope equipped with an ApoTome. Fluorescence-intensity analysis of the digital images was performed using ImageJ software. In separate experiments, flow cytometry was used to evaluate the DC subsets that were bound to the fluorescent peptide. To achieve this aim, the fluorescent CD31 peptide (100 μ g in four dots per mouse) was injected s.c. 1 h before immunization with CFA (Sigma) emulsified in PBS (1:1 vol/vol, 200 μ L in four dots per mouse) at the same skin site. Control mice did not receive CFA immunization. Skin and draining lymph nodes were harvested 1 h and 16 h after the injection of the CD31 peptide and digested in collagenase D (1 mg/mL) diluted in complete medium for 45 min at 37 °C under agitation. The cells were extensively washed with FACS-staining buffer before flow cytometric analysis of DC subsets.

Upholding CD31 During DC Priming with OVA in Vivo. EGFP-Tg mice were injected subcutaneously with 100 μ g of the peptide or the same volume of saline alone, in both flanks, 1 h before subcutaneous immunization, at the same site, with 100 μ g OVA protein (InvivoGen) emulsified in complete Freund's adjuvant. After an overnight period, pooled draining lymph nodes (axillary, brachial, and inguinal) were harvested and digested in collagenase D (1 mg/mL in RPMI; Roche) for 30 min, followed by the addition of 100 mM EDTA and meshing through a 70- μ m filter. The cells were washed, counted, and stained with an allophycocyanin (APC)-conjugated anti-CD11c antibody (clone HL3; BD Biosciences). CD11c^{high} cells from each group of mice were sorted on a BD Biosciences FACSAria III cell sorter in parallel with naive OT-II CD4⁺ T cells (CD4⁺CD62L⁺CD25⁻) and were stained with CTV before being cocultured with sorted OVA-primed DCs (1:10 DC/T cell ratio). Five days later, the culture supernatants were harvested for cytokine analysis by CBA, and the cells were analyzed for proliferation by CTV dilution and for the Treg phenotype (surface CD4/CD25 and intracellular FoxP3 staining, as described below) by flow cytometry. To assess the suppressive functions associated with this phenotype, CD4⁺CD25^{high} cells were FACS-purified from CD31-conditioned OVA-loaded DCs/OT II T-cell cocultures and transferred (2×10^3 CD4⁺CD25^{high} cells per well) in fresh cocultures of CD11c^{high} and naive OT-II CD4⁺ T cells (1:5 ratio, V-bottom, 96-well plates) in the presence of OVA protein (50 μ g/mL). After 5 d of incubation at 37 °C, the supernatant was harvested and analyzed for the content of IFN- γ and IL-10 (CBA).

Adoptive Transfer of CD31-Conditioned DCs. Migration from the skin to draining lymph nodes. BMDCs from C57BL/6 mice were left untouched or stimulated overnight with LPS (1 μ g/mL) with or without CD31 peptide (50 μ g/mL). The cells were then washed and stained with CTV (5 μ M). Recipient mice (three groups: "BMDC"; "BMDC, MOG"; and "CD31 BMDC, MOG") received 100 μ L (administered s.c.) of the appropriate cell suspension (5×10^6 BMDCs per mouse). On the next day, the mice were killed under anesthesia and cell suspensions were prepared from the draining lymph nodes as described previously. The CTV⁺ cells were analyzed by cytometry among the DCs (identified by staining with PE-conjugated anti-CD11c antibody).

Immune function upon antigenic recall challenge in vitro. BMDCs from C57BL/6 mice were either left untouched or incubated with 50 μ g/mL MOG 35–55 peptide (amino acids 35–55, MEVGVYRSPFSRVVHLYRNGK; PolyPeptide Laboratories) during an overnight stimulation with LPS (1 μ g/mL) with or without CD31 peptide (50 μ g/mL), yielding two types of DCs: MOG-loaded mature DCs (BMDC, MOG) and MOG-loaded mature and CD31-conditioned DCs (CD31 BMDC, MOG). Five million cells from each condition were adoptively transferred s.c. into the flanks of C57BL/6 recipient mice, as described above. Ten days after the BMDC adoptive transfer, the draining lymph nodes were harvested, digested, and meshed, and the cells were counted and incubated at 5×10^5 cells per well in 96-well, round-bottom plates with complete medium containing increasing concentrations of MOG 35–55 peptide (up to 200 μ g/mL) for 5 d at 37 °C. The supernatants were thereafter harvested for cytokine analysis.

Immune function upon antigenic recall challenge in vivo (EAE model). Five million each of BMDC; BMDC, MOG; and CD31 BMDC, MOG DCs were adoptively transferred to recipient C57BL/6 mice as described above. A fourth group of mice (no DCs) did not receive exogenous cells ($n = 5$ mice per group, female, 8–10 wk of age). Ten days after DC transfer, EAE was actively induced by immunization with 200 μg of MOG peptide in an emulsion (1:1 by volume) with CFA containing 10 mg/mL heat-inactivated *Mycobacterium tuberculosis* H37RA (Difco Laboratories). A volume of 200 μL of this emulsion was injected s.c. at four sites across the flanks. In addition, 300 ng of pertussis toxin (List Biological Laboratories) was administered to the mice on the same day and again 2 d later. The grid used to monitor the clinical progression of EAE was adapted from Stromnes and Goverman (45). The clinical scores were as follows: 0, no signs; 0.5, partially limp tail; 1, paralyzed tail; 2, hind-limb paresis; 3, one hind limb paralyzed; 4, both hind limbs paralyzed; 5, moribund.

Comparison of immunogenic/tolerogenic properties of untreated and CD31-conditioned BMDCs. BMDCs were prepared as described above, washed, and incubated overnight in complete medium containing LPS (1 $\mu\text{g}/\text{mL}$) and OVA protein (50 $\mu\text{g}/\text{mL}$) and supplemented or not supplemented with the CD31 peptide (100 $\mu\text{g}/\text{mL}$) at a density of 5×10^6 cells per milliliter. Antigen-loaded DCs were thereafter extensively washed with ice-cold PBS, diluted at the indicated concentration, and s.c. injected into C57BL/6 mice that had received, an i.v. bulk of 5×10^5 FACS-purified naive OT-II cells ($\text{CD4}^+\text{CD62L}^+\text{CD25}^-\text{CTV}^+$) 24 h before the injection of the DCs. Five days later, the mice were euthanized and the draining lymph nodes were harvested, meshed, and processed for flow cytometry (CTV dilution, Treg analysis).

Flow Cytometry. Single-cell suspensions (from cultured cells or from freshly harvested lymph nodes) were washed in staining buffer [PBS/1% BSA/2 mM EDTA/0.05% NaN_3 (pH 7.4), 0.22 μm -filtered], incubated with mouse BD Fc block (anti-CD16/32 purified antibodies, 1 $\mu\text{g}/\text{mL}$) for 15 min at 4 $^\circ\text{C}$, and stained with various combinations of fluorescently labeled antibodies directed against CD45 (clone 30-F11, APC), CD4 (clone GK1.5, APC-H7), CD31 (clone MEC 13.3, PE), CD25 (clone PC61, APC), I-A^b (MHCI, clone AF6-120.1, FITC), CD80 (clone 16-10A1, peridinin-chlorophyll protein-Cy 5.5), CD86 (clone GL-1, V450), CD40 (clone 3/23, P APC), CD11c (clone HL3, PE-CF594), CD11b (clone M1/70, PE), CD8 (clone 53-6.7, PerCP), and B220 (clone RA3-6B2, Alexa700) (all from BD Biosciences); Ly6C PE-Cy7 (clone HK1.4, PE-Cy7; Biogegend); MHCI BV421 (clone M5/114.15.2, BV421; Biogegend); CD11c (clone N418, Pacific blue; Invitrogen); and CD103 (clone 2E7, APC; eBiosciences).

Intracellular staining of FoxP3 (PE-conjugated, clone PE-FJK-16; eBiosciences) was performed according to the manufacturer's instructions after the cell surface was stained for CD4 and CD25.

Intracellular IFN- γ and IL-17A were assessed using a Mouse Th1/Th2/Th17 Phenotyping Kit (BD Biosciences) following the manufacturer's instructions.

Intracellular phosphorylation of SHP-2 was assessed in BMDCs incubated at 37 $^\circ\text{C}$ with 200 ng/mL LPS for 15 min in the presence or absence of the CD31 peptide (5×10^6 BMDCs in 100 μL of IMDM per condition). The positive control for CD31-driven SHP-2 phosphorylation was obtained using a rat anti-mouse CD31 antibody (10 $\mu\text{g}/\text{mL}$, clone MEC13.3; BD Biosciences) and goat anti-rat IgG (Fab')₂ fragments (100 $\mu\text{g}/\text{mL}$; Jackson Laboratories). CD31^{-/-} cells were used as the negative control. Intracellular staining with

an anti-SHP-2 (pY542)–PE antibody (clone L99-921; BD Biosciences) or isotype control was performed on fixed/permeabilized cells (BD Phosflow Perm Buffer IV; BD Biosciences) following the manufacturer's instructions.

Cytometric analysis of nuclear NF- κB in LPS-stimulated BMDCs was performed on purified nuclei obtained as described online by the Telford laboratory (<http://home.ccr.cancer.gov/med/flowcore/nuclei.pdf>). Briefly, BMDCs were harvested from the Petri dish and resuspended at a density of 5×10^6 cells per milliliter in IMDM supplemented with 10^{-5} M β -mercaptoethanol, 2 mM L-glutamine, and 1 \times antibiotic/antimycotic solution. The cell suspensions (200 μL) were stimulated with LPS (250 ng/mL) with or without CD31 peptide (50 $\mu\text{g}/\text{mL}$) for 45 min at 37 $^\circ\text{C}$. The cells were then pelleted at 4 $^\circ\text{C}$ ($500 \times g$ for 5 min), washed twice with cold PBS, gently resuspended, and incubated for 10 min on ice in 1 mL of cold nuclear extraction buffer [320 mM sucrose, 5 mM MgCl_2 , 10 mM Hepes, 1% Triton X-100 (pH 7.4)]. Next, the nuclei were pelleted ($2,000 \times g$ for 10 min) and washed twice with cold nuclear wash buffer [320 mM sucrose, 5 mM MgCl_2 , 10 mM Hepes (pH 7.4)]. This extraction procedure provided >98% nuclear purity without any clumping. The nuclei were then incubated for 2 min at room temperature with RNase A (100 U/mL; Qiagen) in nuclear wash buffer, washed, fixed in PBS/4% (wt/vol) PFA for 10 min, and washed twice with nuclear wash buffer. The fixed nuclei were then resuspended in nuclear extraction buffer containing 5 $\mu\text{g}/\text{mL}$ purified polyclonal rabbit anti-mouse NF- κB p65 (no. ab16502; Abcam) and incubated overnight at 4 $^\circ\text{C}$. After two washes in nuclear wash buffer, the secondary antibody (goat anti-rabbit IgG conjugated to Dylight 649, Jackson ImmunoResearch) was added to nuclear extraction buffer supplemented with 0.5% BSA and incubated with the samples for 1 h at room temperature. The nuclei were then washed with nuclear extraction buffer and again with the nuclear wash buffer. Nuclear counterstaining was performed with 1 $\mu\text{g}/\text{mL}$ DAPI in wash buffer supplemented with 0.5% BSA for 5 min. Thereafter, the nuclei were washed extensively, resuspended in wash buffer supplemented with 0.5% BSA, and analyzed. The cytometric acquisition and analysis were performed with an LSRII flow cytometer equipped with three lasers (405, 488, and 633 nm) and BD FACSDiva Software 6.0 (both from BD Biosciences), respectively. Figure-displayed dot plots were obtained using FlowJo software (TreeStar). The data are expressed as arbitrary units [median fluorescence intensity (MFI) normalized against the MFI obtained using the appropriate isotype control].

Statistical Analysis. The results are expressed as the mean \pm SEM. The differences between the groups were evaluated by one-way ANOVA with Fischer's post hoc tests or by Mann-Whitney nonparametric tests as appropriate. Any differences between the groups were considered to be significant when the P value was <0.05 ($*P < 0.05$; $**P < 0.01$). The analysis was performed with JMP 6.0 Software (SAS Institute, Inc.).

ACKNOWLEDGMENTS. We thank Dr. Federica Marelli-Berg for insightful discussions. This work was supported, in part, by the Fondation de France (Grant 2008-002724) and by the Agence Nationale de la Recherche (projects BROSSI and ATHLO). M.C. is the recipient of a doctoral grant provided by the CODDIM from the Region Île de France. G.F. received a grant from the Fondation pour la Recherche Médicale.

- Medzhitov R (2007) Recognition of microorganisms and activation of the immune response. *Nature* 449(7164):819–826.
- Banchereau J, Steinman RM (1998) Dendritic cells and the control of immunity. *Nature* 392(6673):245–252.
- Schumann K, et al. (2010) Immobilized chemokine fields and soluble chemokine gradients cooperatively shape migration patterns of dendritic cells. *Immunity* 32(5):703–713.
- Förster R, et al. (1999) CCR7 coordinates the primary immune response by establishing functional microenvironments in secondary lymphoid organs. *Cell* 99(1):23–33.
- Lutz MB, Schuler G (2002) Immature, semi-mature and fully mature dendritic cells: Which signals induce tolerance or immunity? *Trends Immunol* 23(9):445–449.
- Manicassamy S, Pulendran B (2011) Dendritic cell control of tolerogenic responses. *Immunol Rev* 241(1):206–227.
- Wu J, Horuzsko A (2009) Expression and function of immunoglobulin-like transcripts on tolerogenic dendritic cells. *Hum Immunol* 70(5):353–356.
- Ravetch JV, Lanier LL (2000) Immune inhibitory receptors. *Science* 290(5489):84–89.
- Newman PJ (1999) Switched at birth: A new family for PECAM-1. *J Clin Invest* 103(1):5–9.
- Baumann CI, et al. (2004) PECAM-1 is expressed on hematopoietic stem cells throughout ontogeny and identifies a population of erythroid progenitors. *Blood* 104(4):1010–1016.
- Newton JP, Buckley CD, Jones EY, Simmons DL (1997) Residues on both faces of the first immunoglobulin fold contribute to homophilic binding sites of PECAM-1/CD31. *J Biol Chem* 272(33):20555–20563.
- Brown S, et al. (2002) Apoptosis disables CD31-mediated cell detachment from phagocytes promoting binding and engulfment. *Nature* 418(6894):200–203.
- Hua CT, Gamble JR, Vadas MA, Jackson DE (1998) Recruitment and activation of SHP-1 protein-tyrosine phosphatase by human platelet endothelial cell adhesion molecule-1 (PECAM-1). Identification of immunoreceptor tyrosine-based inhibitory motif-like binding motifs and substrates. *J Biol Chem* 273(43):28332–28340.
- Newton-Nash DK, Newman PJ (1999) A new role for platelet-endothelial cell adhesion molecule-1 (CD31): Inhibition of TCR-mediated signal transduction. *J Immunol* 163(2):682–688.
- Wong MX, Hayball JD, Jackson DE (2008) PECAM-1-regulated signalling thresholds control tolerance in anergic transgenic B-cells. *Mol Immunol* 45(6):1767–1781.
- Fornasa G, et al. (2010) TCR stimulation drives cleavage and shedding of the ITIM receptor CD31. *J Immunol* 184(10):5485–5492.
- Nguyen VA, et al. (2002) Adhesion of dendritic cells derived from CD34+ progenitors to resting human dermal microvascular endothelial cells is down-regulated upon maturation and partially depends on CD11a-CD18, CD11b-CD18 and CD36. *Eur J Immunol* 32(12):3638–3650.
- Fedele G, et al. (2004) CD38 is expressed on human mature monocyte-derived dendritic cells and is functionally involved in CD83 expression and IL-12 induction. *Eur J Immunol* 34(5):1342–1350.
- Ebner S, et al. (1998) Expression of maturation-/migration-related molecules on human dendritic cells from blood and skin. *Immunobiology* 198(5):568–587.
- Carrithers M, et al. (2005) Enhanced susceptibility to endotoxin shock and impaired STAT3 signaling in CD31-deficient mice. *Am J Pathol* 166(1):185–196.
- Maas M, et al. (2005) Endothelial cell PECAM-1 confers protection against endotoxin shock. *Am J Physiol Heart Circ Physiol* 288(1):H159–H164.

22. Graesser D, et al. (2002) Altered vascular permeability and early onset of experimental autoimmune encephalomyelitis in PECAM-1-deficient mice. *J Clin Invest* 109(3):383–392.
23. Tada Y, et al. (2003) Acceleration of the onset of collagen-induced arthritis by a deficiency of platelet endothelial cell adhesion molecule 1. *Arthritis Rheum* 48(11):3280–3290.
24. Newman DK, Hamilton C, Newman PJ (2001) Inhibition of antigen-receptor signaling by Platelet Endothelial Cell Adhesion Molecule-1 (CD31) requires functional ITIMs, SHP-2, and p56(lck). *Blood* 97(8):2351–2357.
25. Sagawa K, Kimura T, Swieter M, Siraganian RP (1997) The protein-tyrosine phosphatase SHP-2 associates with tyrosine-phosphorylated adhesion molecule PECAM-1 (CD31). *J Biol Chem* 272(49):31086–31091.
26. Moraes LA, et al. (2010) Platelet endothelial cell adhesion molecule-1 regulates collagen-stimulated platelet function by modulating the association of phosphatidylinositol 3-kinase with Grb-2-associated binding protein-1 and linker for activation of T cells. *J Thromb Haemost* 8(11):2530–2541.
27. Ramachandran IR, et al. (2011) The phosphatase SRC homology region 2 domain-containing phosphatase-1 is an intrinsic central regulator of dendritic cell function. *J Immunol* 186(7):3934–3945.
28. Rescigno M, Martino M, Sutherland CL, Gold MR, Ricciardi-Castagnoli P (1998) Dendritic cell survival and maturation are regulated by different signaling pathways. *J Exp Med* 188(11):2175–2180.
29. Marelli-Berg FM, Clement M, Mauro C, Caligiuri G (2013) An immunologist's guide to CD31 function in T-cells. *J Cell Sci* 126(Pt 11):2343–2352.
30. Newman PJ, et al. (1990) PECAM-1 (CD31) cloning and relation to adhesion molecules of the immunoglobulin gene superfamily. *Science* 247(4947):1219–1222.
31. Muller WA, Weigl SA, Deng X, Phillips DM (1993) PECAM-1 is required for trans-endothelial migration of leukocytes. *J Exp Med* 178(2):449–460.
32. Muller WA (1995) The role of PECAM-1 (CD31) in leukocyte emigration: Studies in vitro and in vivo. *J Leukoc Biol* 57(4):523–528.
33. Duncan GS, et al. (1999) Genetic evidence for functional redundancy of Platelet/Endothelial cell adhesion molecule-1 (PECAM-1): CD31-deficient mice reveal PECAM-1-dependent and PECAM-1-independent functions. *J Immunol* 162(5):3022–3030.
34. Jackson DE, Gully LM, Henshall TL, Mardell CE, Macardle PJ (2000) Platelet endothelial cell adhesion molecule-1 (PECAM-1/CD31) is associated with a naïve B-cell phenotype in human tonsils. *Tissue Antigens* 56(2):105–116.
35. Ma L, et al. (2010) Ig gene-like molecule CD31 plays a nonredundant role in the regulation of T-cell immunity and tolerance. *Proc Natl Acad Sci USA* 107(45):19461–19466.
36. Wilkinson R, et al. (2002) Platelet endothelial cell adhesion molecule-1 (PECAM-1/CD31) acts as a regulator of B-cell development, B-cell antigen receptor (BCR)-mediated activation, and autoimmune disease. *Blood* 100(1):184–193.
37. Wong MX, Hayball JD, Hogarth PM, Jackson DE (2005) The inhibitory co-receptor, PECAM-1 provides a protective effect in suppression of collagen-induced arthritis. *J Clin Immunol* 25(1):19–28.
38. Yun PL, Decarlo AA, Chapple CC, Hunter N (2005) Functional implication of the hydrolysis of platelet endothelial cell adhesion molecule 1 (CD31) by gingipains of *Porphyromonas gingivalis* for the pathology of periodontal disease. *Infect Immun* 73(3):1386–1398.
39. Sapino A, et al. (2001) Expression of CD31 by cells of extensive ductal in situ and invasive carcinomas of the breast. *J Pathol* 194(2):254–261.
40. Zhang L, et al. (2010) SHP-1 deficient mast cells are hyperresponsive to stimulation and critical in initiating allergic inflammation in the lung. *J Immunol* 184(3):1180–1190.
41. Macatonia SE, Knight SC, Edwards AJ, Griffiths S, Fryer P (1987) Localization of antigen on lymph node dendritic cells after exposure to the contact sensitizer fluorescein isothiocyanate. Functional and morphological studies. *J Exp Med* 166(6):1654–1667.
42. Inaba K, et al. (1992) Generation of large numbers of dendritic cells from mouse bone marrow cultures supplemented with granulocyte/macrophage colony-stimulating factor. *J Exp Med* 176(6):1693–1702.
43. Pfaffl MW (2001) A new mathematical model for relative quantification in real-time RT-PCR. *Nucleic Acids Res* 29(9):e45.
44. Yokomizo T, et al. (2012) Whole-mount three-dimensional imaging of internally localized immunostained cells within mouse embryos. *Nat Protoc* 7(3):421–431.
45. Stromnes IM, Goverman JM (2006) Active induction of experimental allergic encephalomyelitis. *Nat Protoc* 1(4):1810–1819.